2019

Effect of direct current electric field intensity and electrolyte layer thickness on oxygen reduction in simulated atmospheric environment

Xin Zhang

Junxi Zhang

Qimeng Chen

Nianwei Dai

Qingzhao Ni

See next page for additional authors

10.1016/j.corsci.2018.12.013

This is an Author's Accepted Manuscript of: Zhang, X., Zhang, J., Chen, Q., Dai, N., Ni, Q., Zhang, L. -., . . . Zhang, J. (2019). Effect of direct current electric field intensity and electrolyte layer thickness on oxygen reduction in simulated atmospheric environment. *Corrosion Science, 148*, 206-212. Original article available here

Authors
Xin Zhang, Junxi Zhang, Qimeng Chen, Nianwei Dai, Qingzhao Ni, Lai-chang Zhang, Fahe Cao, and Jianqing Zhang

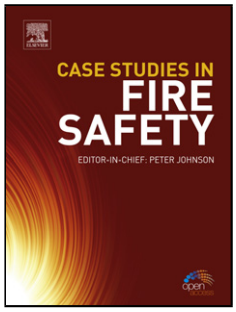

Title: Effect of direct current electric field intensity and electrolyte layer thickness on oxygen reduction in simulated atmospheric environment

Authors: Xin Zhang, Junxi Zhang, Qimeng Chen, Nianwei Dai, Qingzhao Ni, Lai-Chang Zhang, Fahe Cao, Jianqing Zhang

PII: S0010-938X(17)31415-4
DOI: https://doi.org/10.1016/j.corsci.2018.12.013
Reference: CS 7807

To appear in:

Received date: 2 August 2017
Revised date: 5 November 2018
Accepted date: 9 December 2018

Please cite this article as: Zhang X, Zhang J, Chen Q, Dai N, Ni Q, Zhang L-Chang, Cao F, Zhang J, Effect of direct current electric field intensity and electrolyte layer thickness on oxygen reduction in simulated atmospheric environment, *Corrosion Science* (2018), https://doi.org/10.1016/j.corsci.2018.12.013

Effect of direct current electric field intensity and electrolyte layer thickness on oxygen reduction in simulated atmospheric environment

Xin Zhang[a,b], Junxi Zhang[a]*, Qimeng Chen[a], Nianwei Dai[a,c], Qingzhao Ni[a], Lai-Chang Zhang[d*], Fahe Cao[e], Jianqing Zhang[e]

[a]*Key Laboratory of Shanghai Colleges and Universities for Electric Power Corrosion Control and Applied Electrochemistry, Shanghai University of Electric Power, Shanghai 200090, PR China*

[b]*Key Laboratory of Advanced Civil Engineering Materials, Tongji University, Ministry of Education, Shanghai 201804, PR China*

[c]*Department of Materials Science, Fudan University, Shanghai 200433, PR China*

[d]*School of Engineering, Edith Cowan University, 270 Joondalup Drive, Joondalup, Perth, WA 6027, Australia*

[e]*Department of Chemistry, Zhejiang University, Hangzhou, 310027, PR china*

*Corresponding author. E-mail addresses: zhangjunxi@shiep.edu.cn (J. Zhang); l.zhang@ecu.edu.au, lczhangimr@gmail.com (L.C. Zhang).

*Corresponding author: Tel.: +86 1337 1895 961; Fax: +86 21 65700719
E-mail address: zhangjunxi@shiep.edu.cn (J. Zhang); l.zhang@ecu.edu.au, lczhangimr@gmail.com (L.C. Zhang)

Highlights

- Effect of DC electric field on oxygen reduction in TEL was studied.
- Ions migration by DC electric field thermodynamically promotes oxygen

reduction.

- A more negative electrode potential by DC electric field boosts oxygen reduction.
- A model for the effects of the DC electric field on oxygen reduction is proposed.

Abstract:

The effect of direct current (DC) electric field and electrolyte layer thickness on oxygen reduction in simulated atmospheric environment were investigated using electrochemical measurements. The results show that the limiting diffusion current density (i_{lim}) decreases with increasing the thin electrolyte layers (TELs) thickness but it increases with increasing the DC electric field intensity. The potential shifts negatively with the DC electric field. It is found that the DC electric field enables OH^- ions to quickly migrate from the solution/electrode interface to the electrolyte layer. All these features promote the cathodic reduction process thereby enhancing the metal corrosion rate.

Keywords: Electrochemical measurements; Atmospheric corrosion; Oxygen reduction; Thin electrolyte layer (TEL); DC electric field

1. Introduction

Atmospheric corrosion can be considered as wet corrosion of materials under the thin electrolyte layers (TELs) formed on the surface of the material which is an electrochemical process [1]. The anodic process involves the dissolution of metal. Meanwhile, the oxygen reduction reaction is the most important cathodic reaction in atmospheric corrosion.

Considerable endeavours have been made to study the corrosion behaviour of metals in atmospheric environments, including outdoor exposure [2-5] and indoor simulated accelerated experiments [6, 7]. The influences of environmental parameters, such as temperature, humidity [3, 8], chemical compositions of materials [4] and corrosion products [2, 9], on atmospheric corrosion behaviour were extensively studied. In particular, the indoor simulated experiments have been focusing on the mechanism of the correlative factors in the process of metal atmospheric corrosion [6, 7, 10]. Since atmospheric corrosion behaviour is an essentially electrochemical behaviour and such a corrosion behaviour under TELs at later stages depends strongly on the initial corrosion behaviour, it is of importance to study the atmospheric corrosion in TELs at the initial stage using electrochemical methods.

In recent decades, there exist considerable reports on the atmospheric corrosion of metals under TEL systems [11-16]. Some processes can be affected by changing the TEL thickness, such as the mass transport of dissolved oxygen, the hydration of dissolved metal ions and the accumulation of corrosion products [17]. Stratmann et al. [18-20] reported a new technique based on the modified Kelvin Probe to investigate the corrosion behaviour of metals under TELs, by polarisation curves obtained using this new apparatus. Referred to the new apparatus, Nishikata et al [21] for the first time measured the electrochemical properties under TELs by using the electrochemical impedance spectroscopy (EIS) technique and found that the corrosion rate of copper has no relation to the TEL thickness, even under very thin layer thicknesses in Na_2SO_4 solution. In contrast, Liao et al. [22] found that the corrosion rate of copper increases with decreasing the TEL at initial stage. Zhong et al. [23] studied the electrochemical process of a tin electrode under a TEL and also found that the corrosion rate of tin increases with decreasing the TEL thickness at initial stage, due to oxygen diffusion being the main control process. As such, the inhibition effect of the metal cation on the anodic dissolution of tin mitigates the corrosion. Cheng et al. [24] found that the values of oxygen reduction current under a TEL and in the bulk solution were close when the layer thickness is greater than 200 μm, and that the reduction current increased with decrease in the TEL thickness when the thickness was between 200 and 100 μm.

Moreover, studies on the corrosion environments of metals under TELs have been attracting more attention. Corrosion environments of metals is one of the important factors that

affect the corrosion behavior of metals in the TEL. Vera et al. [25] investigated the influence of atmospheric pollutants on the corrosion behaviour of metals and found that high SO_2 concentration resulted in a high corrosion rate. It was also reported that the Cl^- concentration in the TEL has a significant impact on the electrochemical migration (ECM) behaviour of tin. Tin dendrites and precipitates can coexist with each other in low and high chloride concentrations, however, only precipitates but no dendrites were observed at an intermediate Cl concentration [26]. Huang et al. [27] investigated the atmospheric corrosion behaviour for copper printed Circuit Board (PCB-Cu) under a TEL and proposed that the cathodic current density was proportional to the relative humidity. With respect to galvanic corrosion, it was found that the current density and potential distribution of a zinc/steel couple under a TEL were strongly determined by the thickness of the TEL and by the gap between both metals [28]. In addition, Tsai et al. [29] simulated the oxygen transport process in a gas diffusion layer (GDL) of proton exchange membrane fuel cell (PEMFC) using a theoretical model. According to their two-dimensional model, using a thinner GDL could improve the cell performance of PEMFC, indicating that a thicker GDL can result in a higher resistance for oxygen transport toward the electrode surface. Damjanovic and Brusic investigated the electrode kinetics of oxygen reduction on oxide-free platinum electrodes and found a substantial difference in the pH dependence between in acid solution and in alkaline solution [30]. As discussed above, atmospheric corrosion under TELs is very common in different service environments of many metals.

However, it is noted that there are some other important service environments in which metal parts are applied. A significant amount of metal parts subjective to atmospheric corrosion with electric fields is present in transmission towers, substation equipment in power transmission networks as well as in electronic equipment. For example, galvanised steel transmission towers are widely used in China as one of the key parts in power transmission grid. The reliability of a transmission tower is of vital importance to the safety operation of the power transmission grid. In recent years, there exist some reports on the effect of electric fields on the process of metal corrosion [31-36]. Dai et al. [37] studied the atmospheric corrosion behaviour of steel under a DC electric field and proposed that the electric field promotes steel corrosion because it can change the composition and structure of the corrosion products of the

steel. Yuan et al. [38] reported the effects of electric field on the electrochemical process of zinc under a TEL and found that the effects of the DC electric field on the corrosion of zinc could be ascribed to the negative shift of the corrosion potential, increased cathodic polarisation current, and the synergistic effect of the DC electric field and the thickness of the electrolyte layer. These effects can accelerate the cathodic process of metal corrosion. The corrosion behaviour of metals has been studied in soil or in aqueous solution. Preliminary investigations have shown that the corrosion behaviour of metals in electric fields is very different from that in normal conditions. Guo et al. [35, 36] investigated the atmospheric corrosion of copper under a TEL in the application of an electric field and concluded that the effects of electric field on the corrosion of copper under a TEL can be attributed to the effects of electric field on the ion transfer process and oxide film damage. The latest researches [39, 40] suggest that transmission towers corrode at an accelerated rate in an electric field, which is generated around high-voltage transmission lines. Lalvani et al. [31] showed that metal corrosion rate was significantly influenced by the peak potential. Chin et al. [32] and Zhang et al. [33] investigated metal corrosion under an alternating current and found that the corrosion was attributed to the asymmetry of the anodic and cathodic polarisations of the metal. Kim et al. [34] also discussed the effect of an alternating current electric field on metal corrosion and concluded that an external alternating current accelerated the corrosion rate of the metal, thereby destabilising the passive layer. The corrosion behavior of metals in atmospheric environment under the electric field also gets more and more attention. Unfortunately, the effect of the DC electric field on oxygen reduction under TELs has rarely been reported.

The i_{lim} can be used to estimate the maximum value of reaction rate of the oxygen reduction which is controlled by the limiting diffusion process. Electrochemical measurements are considered accurate for determining the i_{lim} value and have been widely used for TELs [1, 22, 28, 41]. Frankel et al. [41] studied the i_{lim} on stainless steel in TELs with the help of electrochemical measurements. Zhang et al. [28] used electrochemical measurements to determine the i_{lim} value of the cathodic reaction on the steel and galvanic corrosion of zinc under a TEL. It was clearly seen that the galvanic current values of zinc and steel in a TEL are related to the thickness of the layer. Liao et al. [22] also used the i_{lim} to describe the corrosion degree of copper in a TEL. Zhang et al. [1] studied the i_{lim} for the cathodic process of iron and

copper under a TEL using electrochemical measurements. According to the above analyses, it is reasonable to believe that electrochemical measurements are an accurate method for determining the i_{lim} value.

In this work, an electrochemical cell was developed to study the effects of the DC electric field and TEL thickness on the i_{lim} value for the oxygen reduction process under a TEL. All these measurements were conducted to achieve further understanding of the atmospheric corrosion of metals under a DC electric field environment.

2. Experimental

2.1. Material preparation and experimental setup

To avoid a large amount of corrosion products having influence on the oxygen reduction, it is appropriate to use Pt as the working electrode instead of other metals. Furthermore, there existed many studies on the oxygen reduction process using Pt [29, 42-44]. The working electrode (WE) was mechanically cut from pure Pt rod (99.9%) and embedded into nylon, leaving a 0.5 cm^2 working area exposed. Prior to testing, the Pt electrode was gradually ground by silicon carbide papers down to 2000 grits, polished with 2.5 μm diamond paste, then, degreased with acetone, rinsed with distilled water and dried in air.

Fig. 1 shows the schematic diagrams of the experimental arrangement for oxygen reduction tests under the DC electric field. This equipment arrangement was improved based on the previous studies on the atmospheric corrosion [18, 20, 22]. A vacuum desiccator with an electrochemical cell was placed on a horizontal stage. The position of the electrochemical cell could be adjusted using a spirit level. The test temperature was 20±0.1 ºC and the relative humidity (RH) was maintained at 60±1%. Specifically, a beaker was placed above the spirit level, into which water-glycerol mixtures were injected in a glycerine and water mixture ratio of 3:1 to obtain the required relative humidity at around 60±1%. The difference between this arrangement and those in previous literature was that a pair of stainless steel plates were set opposite, with a gap of 5 cm, as external electrode plates. The plate on the bottom was grounded with the Pt working electrode, to simulate the ground mode of a transmission tower. The other plate was connected with a high voltage power supply.

A high voltage power supply (DC, LSL-BI, China) was employed to generate stable high voltage (20 kV). With the application of the voltage divider, 4 voltage levels, i.e. 5, 10, 15 and 20 kV, could be distributed to a pair of electrode plates respectively. Correspondingly, a series of DC electric field intensities of 100, 200, 300 and 400 kV/m were obtained. It should be noted that the stability of the DC voltage was good enough to avoid the generation of an induced AC field due to the ripple of the voltage (ripple factor:<0.005%). Furthermore, taking into account the practical DC electric field environment in which the metal was located, the electrode plate on the bottom was connected to the earth-wire through the electrical wire.

The Pt wire with 0.5 mm in diameter acted as the counter electrode and the WE was surrounded by the Pt wire, as shown in Fig. 1(a). It should be noted that a U-shape salt bridge, which was full of 0.35 wt.% NaCl solution, was placed between the WE and RE. A saturated calomel electrode (SCE) was used as the RE. Such a configuration could decrease the Ohmic drop between the WE and RE. After the apparatus was established, the electrolyte was injected in the electrochemical cell and the TEL was formed. The electrolyte used in the experiment was a 0.35 wt.% NaCl solution, which was prepared from deionised water and an analytical reagent NaCl (Sinopharm Chemical Reagent Co., Ltd., Shanghai, China). The pH of the NaCl solution was about 6.8.

The TEL thickness on the Pt electrode surface was determined using a setup which includes a self-designed micrometer (Fig. 1(b)), a Pt needle with a 0.5 mm in diameter and an ohmmeter [20, 22, 23]. The Pt needle was welded on the micrometer. The scale value on the micrometer, based on the position of the Pt needle, was recorded firstly when the Pt needle touched the electrode surface without the electrolyte. A sudden change in the radian on the electrolyte layer could be seen when the Pt needle touched the electrolyte layer and the scale value on the micrometer was recorded again. The difference of both scale values was the value of thickness of the TEL. This technique enabled the TEL thickness measurement to have an accuracy of 5 μm. In this work, the thickness of the TEL was varied between 100 μm and 1000 μm. In addition, a vacuum desiccator with an electrochemical cell was covered with a lid. A cup of NaCl solution of the same concentration as the test solution was placed at the bottom of the vacuum desiccator to maintain the TEL thickness stability during the electrochemical measurements.

2.2. Electrochemical measurements

The potentiodynamic measurements under different TEL thicknesses, with or without the DC electric field, were carried out with a Chi660c electrochemical workstation (Chenhua China). A three-electrode system was used in this experiment. All the potentials were with respect to the SCE. The Pt electrode was covered by the 0.35 wt.% NaCl solution for enough time to make the open circuit potential stable before measurements. The scan range of the potential was from 0.4 to -1.3V at a scan rate of 0.166mV/s. This electrochemical test was performed at room temperature (20±0.1 ^{o}C). All the measurements were repeated at least three times for reproducibility.

In addition, supplementary experiments were done to verify that the potentiodynamic measurements were under steady state diffusion control. The experimental preparation was like the previous one. The potentiodynamic measurements under different TEL thicknesses, with or without the DC electric field, were carried out with a Chi660c electrochemical workstation (Chenhua China). The scan range of the potential was from -0.1 to -1.0V at different scan rates of 0.332, 0.664, 0.996, 1.328, 1.66mV/s. This electrochemical test was performed at room temperature (20±0.1 ^{o}C). All the measurements were repeated at least three times for reproducibility.

3. Results

Fig. 2 show the cathodic polarisation curves of the Pt electrode under various thicknesses of TEL containing 0.35 wt% NaCl under different DC electric field intensities. Each cathodic polarisation curve can be divided into three regions with the negative shift of potential. That is, Region I corresponds to the oxygen reduction controlled by electrochemical polarisation; Region II is the oxygen reduction region controlled by the limiting diffusion process; Region III is attributed to the hydrogen evolution reaction [22]. In Region II, the i_{lim} for dissolved oxygen reduction increases with decreasing the electrolyte thickness.

From the results of the cathodic polarisation of the Pt electrode in the TEL thickness range from 100 μm to 1000 μm under different DC electric field intensities, the smaller the thickness

of the electrolyte layer is, the higher the value of the i_{lim} is. When the electrolyte thickness is higher than 300 μm, slight changes are found for the i_{lim}. On the contrary, significant changes are found when the electrolyte thickness is less than 300 μm. These results are in good agreement with those reported in Ref [28]. Usually, the i_{lim} value is a function of inverse solution thickness, according to the Nernst-Fick equation [1, 20, 28, 41]:

$$i_{lim} = \frac{nFDC}{d_{soln}} \quad (1)$$

where i_{lim} is the limiting diffusion current density; n represents the number of electrons in the oxygen reduction; F is the Faraday constant; D is the diffusion constant; C represents the concentration of dissolved oxygen and d_{soln} is the solution layer thickness. The number of the electrons in the oxygen reduction process is 4; the value of dissolved oxygen concentration in 0.35% NaCl solution is 1.95×10^{-4} mol/l [45] and the oxygen diffusion coefficient 1.9×10^{-5} cm^2s^{-1} (20 °C) [28]. Therefore, the value of the i_{lim} can be calculated based on the Nernst-Fick equation.

Fig. 3 shows the relations between the i_{lim} and $1/d_{soln}$ with various DC electric field intensities. This figure includes the calculated values based on the Nernst-Fick equation and the measured values according to the cathodic polarisation curves under different TEL thicknesses without DC electric field. For thicker TELs, with the TEL thickness of from 400 μm (i.e. $1/d_{soln}$=0.0025) to 1000 μm (i.e. $1/d_{soln}$=0.001), the measured values gradually deviate from the calculated one under a TEL thickness of more than 300 μm (i.e. $1/d_{soln}$=0.0033). In contrast, the calculated value agrees well with the measured one for thinner TELs less than 300 μm (i.e. $1/d_{soln}$=0.0033). One obtains 300 μm as the effective diffusion layer thickness in TEL based on the above experimental results. This is in good agreement with the previous results in Ref [28]. When the TEL thickness is less than the effective diffusion layer thickness, the measured value is close to the calculated one. When the TEL thickness is higher than the effective diffusion layer thickness, the measured value has the more deviation from the calculated one. Moreover, it is obvious that the i_{lim} increases with increasing the DC electric field intensity (Fig. 3). For example, when the thickness is 400 μm without the DC electric field, i_{lim} is about 45 $\mu A\cdot cm^{-2}$; the i_{lim} value reaches 52 $\mu A\cdot cm^{-2}$ when the DC electric field intensity is 100 kV/m; and when the DC electric field intensity is increased to 400 kV/m, the i_{lim} reaches 89 $\mu A\cdot cm^{-2}$.

Fig. 4 presents the relationship between the effect of different DC electric field intensities and the various TEL thicknesses, which is fitted from the dependence of the i_{lim} on the DC electric field intensities under various TEL thicknesses (Fig. 4 inset). In general, the slope value (di_{lim}/dE) represents the effect of the DC electric field intensities. It can be clearly seen that the di_{lim}/dE value decreases as the TEL thickness increases. It is interesting to note that the increased rate of (di_{lim}/dE) is prominent when the TEL thickness is less than 300 μm. Meanwhile, the (di_{lim}/dE) value exhibits a high value when the thickness is less than 300 μm but a low value when the TEL thickness is greater than 300 μm.

Fig. 5 (a-c) show the cathodic polarisation curves at different scan rates under different TEL with various DC electric field intensities. It is prominent that under TEL of 100μm and 600μm without the DC electric field, the value of current density(i_{lim}) is independent of the sweep rate. It is the same in the condition of TEL of 400μm with the DC electric field of 100kV/m. That is, these potentiodynamic measurements of different scan rates under different TEL with various DC electric field intensities are all under steady state diffusion control.

4. Discussion

4.1. Oxygen reduction under the TEL without the DC electric field

As obtained in Fig. 2, the results from cathode polarisation curves show that the i_{lim} increases as TEL thickness decreases under no DC electric field. This is in good agreement with the conclusions by other researchers [1, 28, 41]. The i_{lim} increases significantly when the thickness is less than 300 μm. As for thicker TELs, when TEL thickness is higher than the effective diffusion layer thickness (300 μm), the i_{lim} varies somewhat (Fig. 3). Stratmann et al. [20] reported that the oxygen diffusion from the electrolyte layer to the electrolyte/electrode interface is the rate determining step in thinner TELs. Zhang et al. [1] pointed out that the i_{lim} value for the cathodic process depends on the TEL thickness when the thicknesses are greater than 100 μm. It was also reported that the reduction rate of O_2 is affected by the change in electrolyte thickness, when the thickness of the TEL is less than the diffusion layer thickness [28]. As illustrated in Fig. 2 and Fig. 3, the smaller the TEL thickness is, the higher the i_{lim} is for TEL thicknesses less than 300 μm. Based on these results, it is reasonable to believe that for

TEL thicknesses close to or less than the effective diffusion layer thickness, the dependence of the i_{lim} on the TEL thickness is attributed to the effect of the changes in TEL thickness on the oxygen transfer rate. As observed in Fig. 2, the reduction reaction is controlled by the diffusion of oxygen to the electrode surface. In other words, when the TEL thickness is near or less than the effective diffusion layer thickness, the oxygen reduction rate is dependent on the diffusion rate of oxygen through the TEL [1, 20, 28].

4.2. Oxygen reduction under the TEL with the DC electric field

As seen in Fig. 2 and Fig. 3, the application of the DC electric field enhances the i_{lim}. Oxygen reduction is the main process in the cathodic polarisation curve [1, 25, 41]. Meanwhile, oxygen reduction reaction including some processes is controlled by diffusion process in solution system. But in the thin electrolyte layer, oxygen transmission turns to one-dimensional transmission when the TEL thickness of electrolyte layer is smaller. So the kinetic process of oxygen reduction reaction in the thin electrolyte layer changes greatly compared with that in the usual solution system. The equation for oxygen reduction is:

$$2H_2O+O_2+4e \rightarrow 4OH^- \quad (2)$$

With the effect of the DC electric field, the anion OH^- can migrate from the electrode surface to the layer surface. According to thermodynamic principles, it can also accelerate the reduction of oxygen when the OH^- anions transfer out of the solution/electrode interface more quickly with the DC electric field, thereby increasing the i_{lim} value. As seen in Fig. 3, for the same thickness, the higher the DC electric field intensities, the higher the i_{lim} value. This means the electric field can influence the oxygen reduction under TELs by promoting the relevant shift of ions out of the electrode/solution interface. The migration rate is faster with the addition of increased DC electric field intensity [46]. Dai et al. [37] pointed out that the DC electric field breaks the coexistence of ions in the electrode/solution interface, and the shift of the anion away from the electrode/solution interface is favourable for loose corrosion product. As can be seen in the cathodic polarisation curves (Fig. 2), the thinner the thickness of the electrolyte layer, the higher the current of the oxygen reduction. The related content of migration of OH^- ion that is referred to is from the view point of thermodynamics. The OH^- ions derived from the reduction

of oxygen can increase the reduction of dissolved oxygen in thermodynamic. Therefore, the concentration of OH^- ion can affect the reduction of dissolved oxygen. Thus, it is believed that the higher the DC electric field intensity, the more OH^- ions shift out of the electrode/solution interface therefore the higher the i_{lim} value.

On the other hand, the evolution of electrode potential value from the cathodic polarisation curves under TELs of various thicknesses with different DC electric field intensities can be seen from Fig. 6. It is remarkable that little change occurred to the electrode potential value in TELs under weaker DC electric field intensity (0-100kV). When the DC electric field intensity is higher than 200 kV/m, the electrode potential shifts negatively with increasing the DC electric field intensities. Meanwhile, in the same DC electric field intensities, for thicker TELs from 400 μm to 1000 μm, the change in the TEL thickness has weaker influence on the potential value. By contrast, for thinner TELs (100-300 μm), the thinner the TEL thickness is, the more negative the electrode potential can be. Huang et al. [36] reported that the potential shifted negatively in the electric field because of the imbalance between the anode and the cathode processes. It is pointed out that the charge density at the electrode/solution interface may increase when the DC electric field is exerted. As a result, the electrode potential can be shifted negatively [38]. With increasing the DC electric field intensity, the charge density at the electrode/solution interface may increase. As a result, the electrode potential becomes more negative. Therefore, oxygen reduction could be performed further, and more OH^- ions are produced. With the decrease in the TEL thickness, the concentration of OH^- in the TEL is increased. Thus, the value of pH of the TEL become larger. According to the Pourbaix diagram, the higher the concentration of OH^- is, the more negative the electrode potential is. These results explain why the electrode potential of the Pt electrode becomes negative with decreasing the TEL thickness for those cases with thinner TELs. By contrast, for thicker TELs, the change in the TEL thickness has little influence on the potential value.

4.3. Ideal model for the effect of the DC electric field on oxygen reduction

On account of the above results, a model for the effects of the DC electric field on oxygen reduction is thus proposed. Fig. 7 shows a schematic illustration of the distribution of ions in the

electrode/TEL system with and without the DC electric field. As seen from Fig. 7, the H^+ cations migrate to the negative pole while the OH^- anions migrate in the opposite direction under the DC electric field. Based on Equ. (2), the OH^- anions transfer out of the solution/electrode interface more quickly with the application of the DC electric field. As a result, the oxygen cathodic reduction process can be accelerated. Therefore, the i_{lim} value increases with increasing the DC electric field intensity.

Alternatively, as can be seen in Fig. 6, when the TEL thickness is small, the electrode potential under a strong DC electric field can be shifted negatively. It is believed that the charge density at the electrode/solution interface may increase with the application of the DC electric field, which can result in a more negative electrode potential. Then, the negative shift of the electrode potential promotes the reduction of the cathodic process [38], suggesting that the i_{lim} value can rise. Based on these results, the ideal model for the effects of the DC electric field on the oxygen reduction in the TEL can be expressed in two factors. The first factor is that the distribution change of the ions (the major ion is OH^-) promotes the oxygen reduction in the TEL. The second one is that the oxygen reduction process can be accelerated by shifting the electrode potential negatively in the thin TEL. To be more exact, for thicker TELs (400-1000 μm), the DC electric field has little effect on the i_{lim} value. In contrast, for thinner TELs less than 300 μm, the i_{lim} value is significantly influenced by the DC electric field. These results are in well agreement with the results obtained from Fig. 4.

5. Conclusions

The limiting current density value (i_{lim}) is shown to increase by potentiodynamic measurements with the addition of direct current (DC) electric field intensity under thin electrolyte layers (TELs). The results show that the oxygen reduction on the Pt electrode is enhanced with the application of DC electric field under the TEL. For thicker TELs, the increasing rate of the i_{lim} value is low and the DC electric field accelerates the oxygen reduction process on the Pt electrode under the thicker TEL due to the separation of the OH^- ions. By contrast, for thinner TELs, the separation of the OH^- ions and the negative shift of the electrode potential can work together, thereby accelerating the oxygen reduction process on the Pt

electrode. So, the increasing rate of the i_{lim} value is high. When the ions quickly migrate out from the solution/electrode interface to the TEL surface and the electrode potential becomes more negative with the existence of DC electric field, the oxygen cathodic reduction process can be accelerated, resulting in a higher metal corrosion rate.

Acknowledgements

The authors acknowledge financial support from the National Natural Science Foundation of China (No. 51271110) and the Science Research Foundation of Shanghai Education Committee (12ZZ170). We thank proofreading (www.proof-reading-service.com) for its linguistic assistance during the preparation of this manuscript.

References

[1] S. H. Zhang, S. B. lyon, The electrochemistry of iron, zinc and copper in thin layer electrolytes, Corros. Sci. 35 (1993) 713-718.

[2] R. A. Antune, I. Costa, D. L. A. d. Faria, Characterization of Corrosion Products formed on steels in the first months of atmospheric exposure, Mater. Res. 6 (2003) 403-408.

[3] J. Morales, F. Díaz, J. Hernández-Borges, S. González, V. Cano, Atmospheric corrosion in subtropical areas: Statistic study of the corrosion of zinc plates exposed to several atmospheres in the province of Santa Cruz de Tenerife (Canary Islands, Spain), Corros. Sci. 49 (2007) 526-541.

[4] J. Liao, M. Hotta, Atmospheric corrosion behavior of field-exposed magnesium alloys: Influences of chemical composition and microstructure, Corros. Sci. 100 (2015) 353-364 .

[5] W. Han, C. Pan, Z. Wang, G. Yu, A study on the initial corrosion behavior of carbon steel exposed to outdoor wet-dry cyclic condition, Corros. Sci. 88 (2014) 89-100.

[6] R. P. V. CRUZ, A. NishIkata, T. tsuru, AC impedance monitoring of pitting corrosion of stainless steel under a wet-dry cyclic condition in chloride-containing environment, Corros. Sci. 38 (1996) 1397-1406.

[7] B. Qian, B. Hou, M. Zheng, The inhibition effect of tannic acid on mild steel corrosion in seawater wet/dry cyclic conditions, Corros. Sci. 72 (2013) 1-9.

[8] S. Syed, Atmospheric corrosion of hot and cold rolled carbon steel under field exposure in Saudi Arabia, Corros. Sci. 50 (2008) 1779-1784.

[9] J. D. Yoo, K. Ogle, P. Volovitch, The effect of synthetic zinc corrosion products on corrosion of electrogalvanized steel. II. Zinc reactivity and galvanic coupling zinc/steel in presence of zinc corrosion products, Corros. Sci. 83 (2014) 32-37.

[10] J. Chen, J. Wang, E. Han, W. Ke, In situ observation of formation and spreading of micro-droplets on magnesium and its alloy under cyclic wet–dry conditions, Corros. Sci. 49 (2007) 1625-1634.

[11] H. Katayama, S. Kuroda, Long-term atmospheric corrosion properties of thermally sprayed Zn, Al and Zn–Al coatings exposed in a coastal area, Corros. Sci. 76 (2013) 35-41 .

[12] J. Monnier, S. Réguer, E. Foy, D. Testemale, F. Mirambet, M. Saheb, P. Dillmann, I. Guillot, XAS and XRD in situ characterisation of reduction and reoxidation processes of iron corrosion products involved in atmospheric corrosion, Corros. Sci. 78 (2014) 293-303.

[13] T. H. Muster, A. Bradbury, A. Trinchi, I. S. Cole, T. Markley, D. Lau, S. Dligatch, A. Bendavid and P. Martin, The atmospheric corrosion of zinc: The effects of salt concentration, droplet size and droplet shape, Electrochim. Acta. 56 (2011) 1866-1873.

[14] V. Ligier, M. Wéry, J.-Y. Hihn, J. Faucheu, M. Tachez, Formation of the main atmospheric zinc end products: $NaZn_4Cl(OH)_6SO_4 \cdot 6H_2O$, $Zn_4SO_4(OH)_6 \cdot nH_2O$ and $Zn_4Cl_2(OH)_4SO_4 \cdot 5H_2O$ in [Cl^-] [SO_42^-] [HCO^{3-}] [H_2O_2] electrolytes, Corros. Sci. 41 (1999) 1139-1164.

[15] V. Barranco, S. Feliu Jr, S. Feliu, EIS study of the corrosion behaviour of zinc-based coatings on steel in quiescent 3% NaCl solution. Part 1: directly exposed coatings, Corros. Sci. 46 (2004) 2203-2220.

[16] T. Prosek, D. Thierry, C. Taxén, J. Maixner, Effect of cations on corrosion of zinc and carbon steel covered with chloride deposits under atmospheric conditions, Corros. Sci. 49 (2007) 2676-2693.

[17] A. Nishikata, Y. Ichihara, Y. Hayashi, T. Tsuru, Influence of electrolyte layer thickness and pH on the initial stage of the atmospheric corrosion of iron, J. Electrochem. Soc 144 (1997) 1244-1254.

[18] M. Stratmann, H. Streckel, On the atmospheric corrosion of metals which are covered with thin electrolyte layers—I. Verification of the experimental technique, Corros. Sci. 30 (1990)

681-696.

[19] M. Stratmann, H. Streckel, On the atmospheric corrosion of metals which are covered with thin electrolyte layers—II. Experimental results, Corros. Sci. 30 (1990) 697-714.

[20] M. Stratmann, H. Streckel, K. T. KIM, S. Crockett, On the atmospheric corrosion of metals which are covered with thin electrolyte layers-iii. the measurement of polarisation curves on metal, Corros. Sci. 30 (1990) 715-734.

[21] A. Nishikata, Y. Ichihara, T. Tsuru, An application of electrochemical impedance spectroscopy to atmospheric corrosion study, Corros. Sci. 37 (1995) 897-911.

[22] X. Liao, F. Cao, L. Zheng, W. Liu, A. Chen, J. Zhang, C. Cao, Corrosion behaviour of copper under chloride-containing thin electrolyte layer, Corros. Sci. 53 (2011) 3289-3298.

[23] X. Zhong, G. Zhang, Y. Q iu, Z. Chen, X. Guo, C. Fu, The corrosion of tin under thin electrolyte layers containing chloride, Corros. Sci. 66 (2013) 14-25.

[24] Y. L. Cheng, Z. Zhang, F. H. Cao, J. F. Li, J. Q. Zhang, J. M. Wang, C. N. Cao, A study of the corrosion of aluminum alloy 2024-T3 under thin electrolyte layers, Corros. Sci. 46 (2004) 1649-1667.

[25] R. Vera, D. Delgado, B. M. Rosales, Effect of atmospheric pollutants on the corrosion of high power electrical conductors: Part 1. Aluminium and AA6201 alloy, Corros. Sci. 48 (2006) 2882-2900.

[26] X. Zhong, G. Zhang, Y. Qiu, Z. Chen, X. Guo, Electrochemical migration of tin in thin electrolyte layer containing chloride ions, Corros. Sci. 74 (2013) 71-82.

[27] H. Huang, Z. Dong, Z. Chen, X. Guo, The effects of Cl^- ion concentration and relative humidity on atmospheric corrosion behaviour of PCB-Cu under adsorbed thin electrolyte layer, Corros. Sci. 53 (2011) 1230-1236.

[28] X. G. Zhang, E. M. Valeriote, Galvanic protection of steel and galvanic corrosion of zinc under thin layer electrolytes, Corros. Sci. 34 (1993) 1957-1972.

[29] C. R. Tsai, F. Chen, A. C. Ruo, M.-H. Chang, H.-S. Chu, C. Y. Soong, W. M. Yan and C. H. Cheng, An analytical solution for transport of oxygen in cathode gas diffusion layer of PEMFC, J. Power Sources. 160 (2006) 50-56.

[30] A. Damjanovic, V. Brusic, Electrode kinetics of oxygen reduction on oxide-free platinum electrodes, Electrochim. Acta. 12 (1967) 615-628.

[31] S. B. Lalvani, G. Zhang, The corrosion of carbon steel in a chloride environment due to periodic voltage modulation: Part II, Corros. Sci. 37 (1995) 1583-1598.

[32] J. L. Wendt, D. T. Chin, The a.c. corrosion of stainless steel—II. The breakdown of passivity of ss304 in neutral aqueous solutions, Corros. Sci. 25 (1985) 889-900.

[33] J. Zhang, J. Yuan, Y. Qiao, C. Cao, J. Zhang, G. Zhou, The corrosion and passivation of SS304 stainless steel under square wave electric field, Mater. Chem. Phys. 79 (2003) 43-48.

[34] D.-K. Kim, S. Muralidharan, T.-H. Ha, J.-H. Bae, Y.-C. Ha, H.-G. Lee, J. D. Scantlebury, Electrochemical studies on the alternating current corrosion of mild steel under cathodic protection condition in marine environments, Electrochim. Acta. 51 (2006) 5259-5267.

[35] J. Toribio, V. Kharin, M. Lorenzo, D. Vergara, Role of drawing-induced residual stresses and strains in the hydrogen embrittlement susceptibility of prestressing steels, Corros. Sci. 53 (2011) 3346-3355.

[36] H. Huang, Z. Pan, X. Guo, Y. Qiu, Effect of an alternating electric field on the atmospheric corrosion behaviour of copper under a thin electrolyte layer, Corros. Sci. 75 (2013) 100-105.

[37] N. Dai, J. Zhang, Q. Chen, B. Yi, F. Cao, J. Zhang, Effect of the direct current electric field on the initial corrosion of steel in simulated industrial atmospheric environment, Corros. Sci. 99 (2015) 295-303 .

[38] X. J. Yuan, J. X. Zhang, Q. M. Cheng, T. Tan, X. C. Ma, Electrochemical Process of Zn Electrode Covered with Thin Electrolyte Layer under External Electric Field, Corros. Sci. Prot. Technol. 26 (2014) 197-204.

[39] X. J. Yuan, J. X. Zhang, Q. Chen, S. M. Zhang, T. Tan, Corrosion behavior of zinc covered with thin electrolyte layers under external electric field, J. Electroanal. Chem. 19 (2013) 430-436.

[40] N. Dai, Q. Chen, J. Zhang, X. Zhang, Q. Ni, Y. Jiang, J. Li, The corrosion behavior of steel exposed to a DC electric field in the simulated wet-dry cyclic environment, Mater. Chem. Phys. 192 (2017) 190-197.

[41] G. S. Frankel, M. Stratmann, M. Rohwerder, A. Michalik, B. Maier, J. Dora, M. Wicinski, Potential control under thin aqueous layers using a Kelvin Probe, Corros. Sci. 49 (2007) 2021-2036.

[42] J. Chen, T. Matsuura, M. Hori, Novel gas diffusion layer with water management function

for PEMFC, J. Power Sources. 131 (2004) 155-161.

[43] H.-K. Lee, J.-H. Park, D.-Y. Kim, T.-H. Lee, A study on the characteristics of the diffusion layer thickness and porosity of the PEMFC, J. Power Sources. 131 (2004) 200-206.

[44] H. Dohle, A. A. Kornyshev, A. A. Kulikovsky, J. Mergel, D. Stolten, The current voltage plot of PEM fuel cell with long feed channels, Electrochem. Commun. 3 (2001) 73-80.

[45] A. J. van Stroe, L. J. J. Janssen, Determination of the diffusion coefficient of oxygen in sodium chloride solutions with a transient pulse technique, Anal. Chim. Acta. 279 (1993) 213-219.

[46] H. Huang, X. Guo, G. Zhang, Z. Dong, The effects of temperature and electric field on atmospheric corrosion behaviour of PCB-Cu under absorbed thin electrolyte layer, Corros. Sci. 53 (2011) 1700-1707.

Figures:

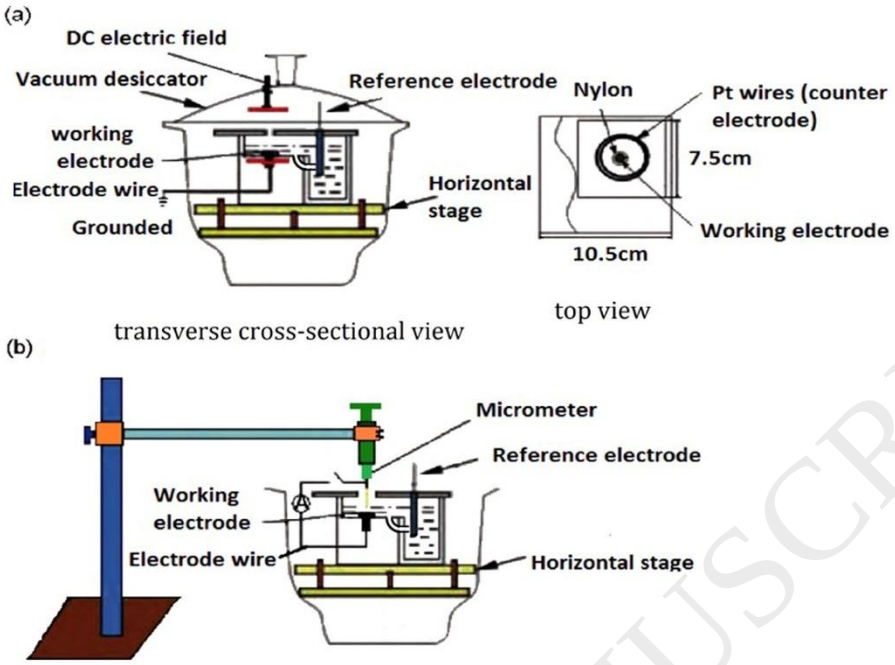

Fig. 1. Schematic diagrams of the experimental apparatus for oxygen reduction testing under DC electric field: (a) the electrochemical measurement in the TEL and (b) the determination of TEL thickness.

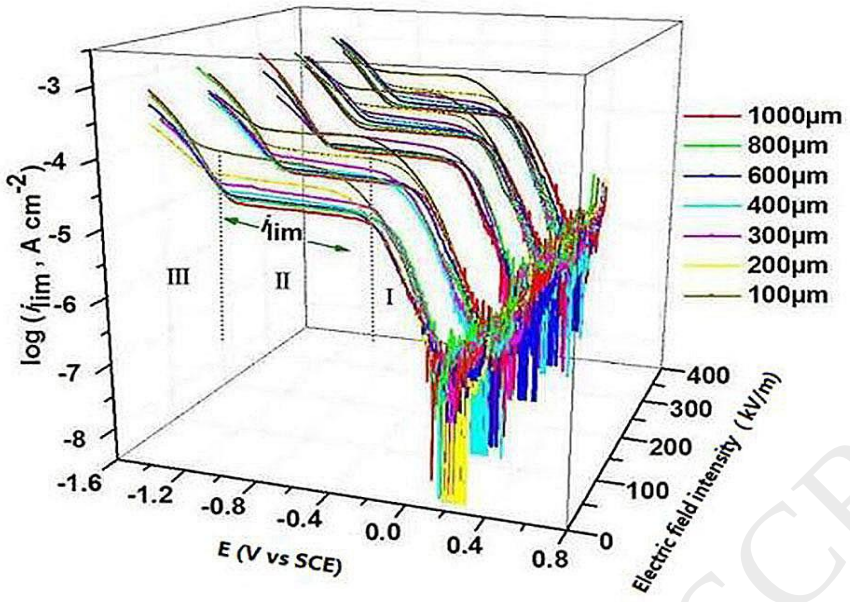

Fig. 2. Cathodic polarisation curves of the Pt electrode with various thicknesses of TEL, containing 0.35 wt% NaCl, at different DC electric field intensities.

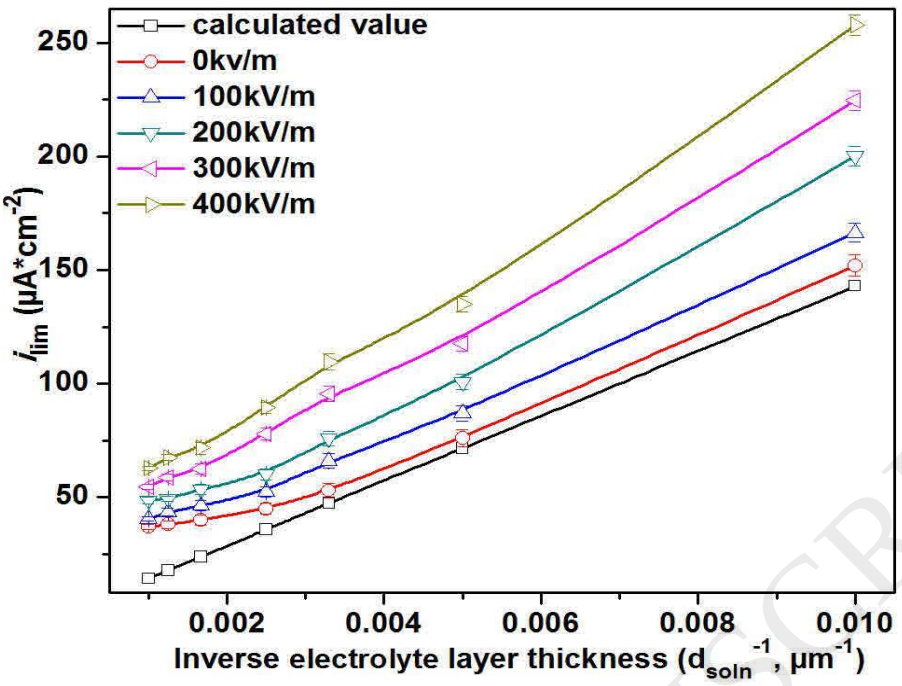

Fig. 3. Dependence of the limiting current density, i_{lim}, on the inverse solution layer thickness at various DC electric field intensities.

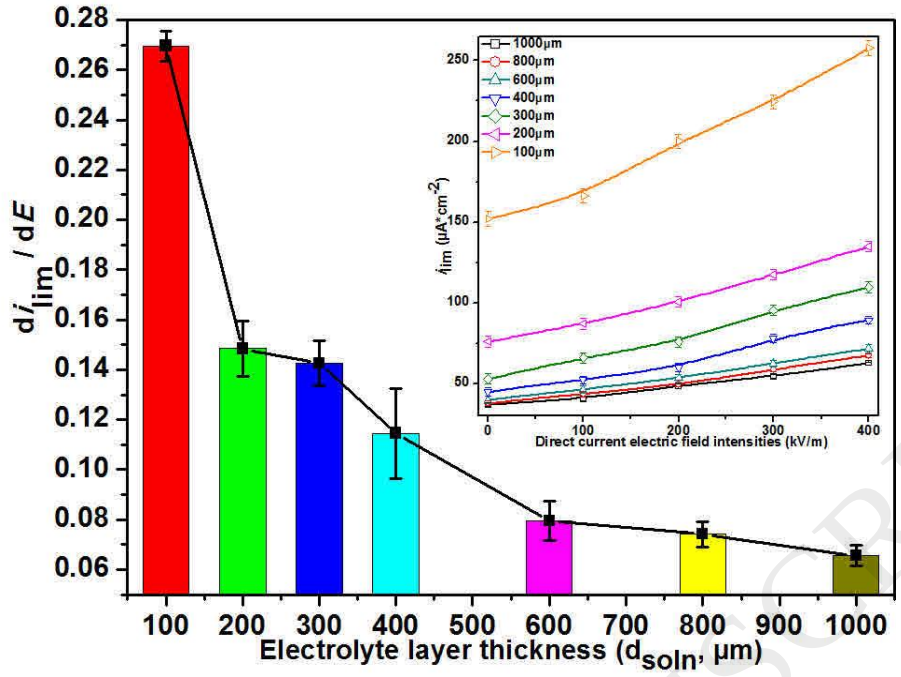

Fig. 4. The effect of DC electric field di_{lim}/dE as a function of TEL thickness.

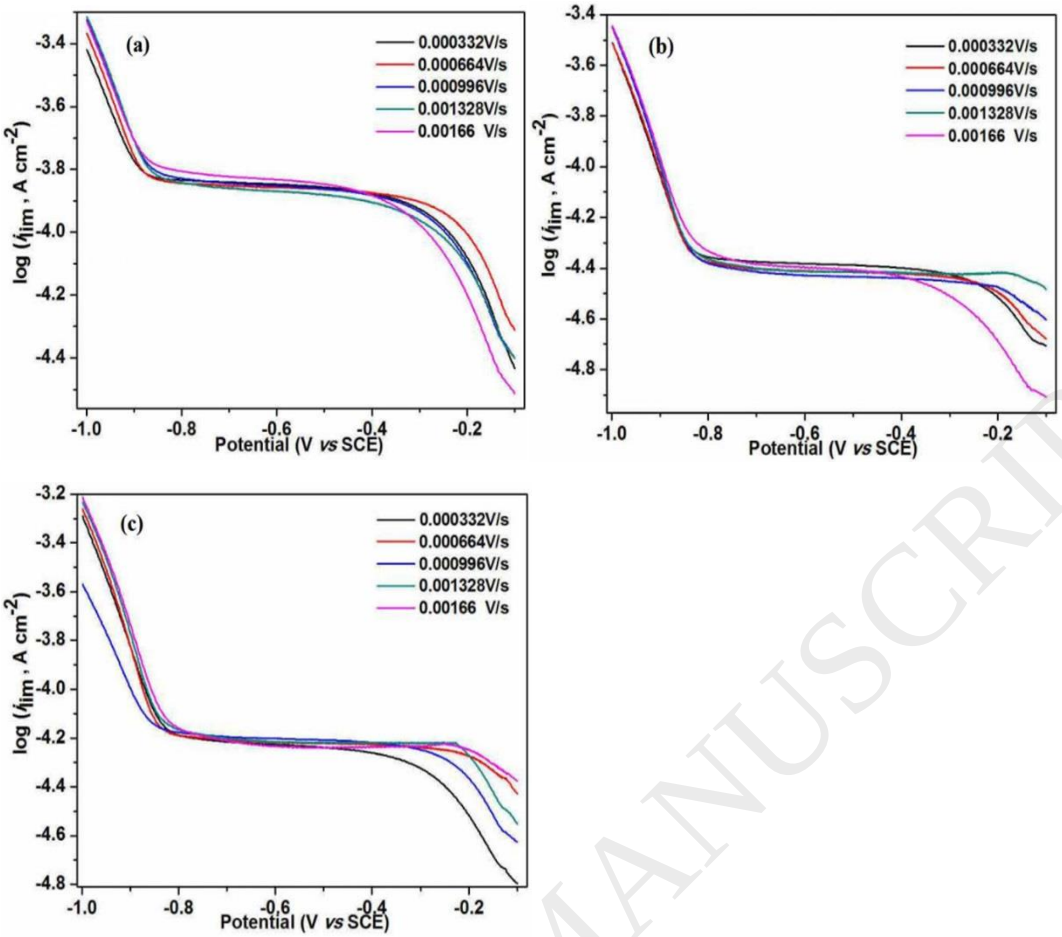

Fig. 5. Cathodic polarisation curves of different scan rates under different TEL thickness with various DC electric field intensities: (a) 100µm without the DC electric field, (b) 600µm without the DC electric field, (c) 400µm with the DC electric field of 100kV/m

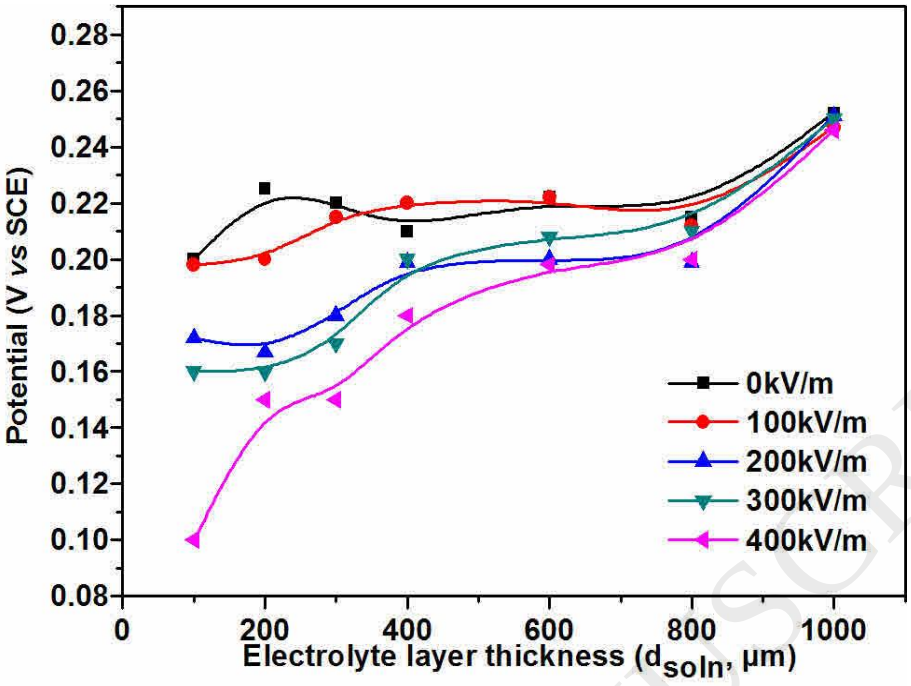

Fig. 6. Evolution of electrode potential value from the cathodic polarisation curves under TELs of various thicknesses at different DC electric field intensities.

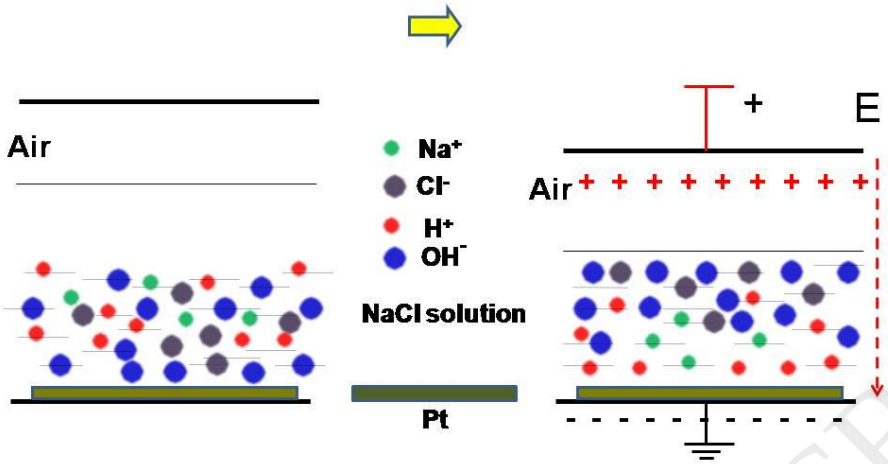

Fig. 7. Schematic illustrations of the migration of ions in a TEL: (a) without the DC electric field and (b) with the DC electric field.